RESEARCH ARTICLE

Molecular Mechanism Underlying Hesperetin-induced Apoptosis by *in silico* Analysis and in Prostate Cancer PC-3 Cells

Shanmugam Sambantham[1], Mahendran Radha[1,2], Arumugam Paramasivam[1], Balakrishnan Anandan[1], Ragunathan Malathi[1], Samuel Rajkumar Chandra[1]*, Gopalswamy Jayaraman[1]

Abstract

Aim: To investigate the molecular mechanisms underlying triggering of apoptosis by hesperetin using *in silico* and *in vitro* methods. Methods: The mechanism of binding of hesperetin with NF-κB and other apoptotic proteins like BAX, BAD, BCL_2 and BCL_{XL} was analysed *in silico* using Schrodinger suite 2009. *In vitro* studies were also carried out to evaluate the potency of hesperetin in inducing apoptosis using the human prostate cancer PC-3 cell line. Results: Hesperetin was found to exhibit high-affinity binding resulting from greater intermolecular forces between the ligand and its receptor NF-κB (-7.48 Glide score). *In vitro* analysis using MTT assay confirmed that hesperetin reduced cell proliferation (IC_{50} values of 90 and 40μM at 24 and 48h respectively) in PC-3 cells. Hesperetin also downregulated expression of the anti-apoptotic gene BCL_{XL} at both mRNA and protein levels and increased the expression of pro-apoptotic genes like *BAD* at mRNA level and *BAX* at mRNA as well as protein levels. Conclusion: The results suggest that hesperetin can induce apoptosis by inhibiting NF-κB.

Keywords: Docking - hesperetin - apoptosis - *NF-κB*

Asian Pac J Cancer Prev, **14 (7)**, 4347-4352

Introduction

Cancer is caused by unregulated cell proliferation and it is the leading cause of death both in developed and in developing countries. About 12.7 million new cancer cases and 7.6 million cancer related deaths were estimated to have occurred in 2008 worldwide (Jemal et al., 2011). Numerous modalities for treatment of cancer are available for cancer such as radiation therapy, chemotherapy, surgery, immunotherapy and hormonal therapy, but nutritional therapy is proving to be a promising treatment option. Many researches are attempted on plant metabolites like flavonoids such as curcumin, taxol, genestin etc. Hesperetin, a citrus flavanone (3, 5, 7-trihydroxy-4-methoxy-flavanone) (Figure 1) has been reported to possess many medicinal properties including blood lipid lowering activity (Borradaile et al., 1999), free radical scavenging (Orallo et al., 2004; Leelavinothan and Kalist, 2011), antioxidant (Choi, 2008) and anti-carcinogenic activities (Tanaka et al., 1997). This compound has been shown to inhibit DMBA induced mammary carcinoma in rats (So et al., 1997). It exerted anti-proliferative effect on MCF-7 breast cancer cell line (Choi, 2007). It also exhibited potent beneficial role against DMH-induced colon carcinogenesis, by inhibiting cell proliferation and angiogenesis and by inducing apoptosis in cancer cells (Nalini et al., 2012).

Reports on the mechanism underlying induction of apoptosis by hesperetin are not available. The conventional methods to identify the molecular mechanism of action of cancer drugs are very tedious and time consuming. On the other hand, computational-based methodologies have proved to be efficient and inexpensive tools. The computational strategies for determining protein targets of flavonoids including hesperetin have not yet received a great deal of attention. The present study aimed to employ computational molecular docking and *in vitro* assays using PC-3 human prostate cancer cell line to determine the effective target for hesperetin

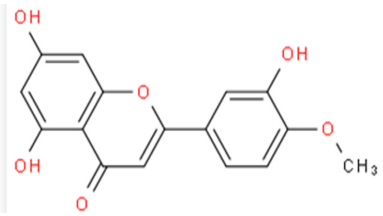

Figure 1. Structure of Hesperetin

[1]*Department of Genetics, Dr.ALMPGIBMS, University of Madras,* [2]*Department of Bioinformatics, Vels University, Chennai, India*
**For correspondence: nchandrarsamuel@gmail.com*

Materials and Methods

Docking studies

The molecular docking involves four steps: *i*) Ligand preparation, the ligand hesperetin was created and energy minimized using LigPrep module of Schrodinger suite version 9 keeping one conformer per ligand, and rest of the parameters were kept as default; *ii*) Protein preparation, the crystal structure of pro- and anti-apoptotic proteins BAX (PDB ID: 1F16), BAD (1G5J), BCL_2 (2O2F), BCL_{XL}(1R2D) and NF-κB (1SVC) was retrieved from Protein Data Bank and for FADD the structure was predicted using Schrodinger software suite (version 9). All the target proteins were prepared using Protein preparation wizard in Maestro; *iii*) Glide grid generation, glide searches for favourable interaction between the ligand molecules and a receptor molecule usually a protein. The shape and properties of the receptor (proteins) are represented on a grid by several different sets of fields that provide more accurate scoring of the ligand pose which is the position and orientation relative to the receptor. and *iv*); Docking was performed by using the Glide 5.5 integrated with Maestro 9 (Schrodinger, LLC, 2009). The structure of human BCL_2 (2O2F), BCL_{XL} (1R2D), BAX (1F16), BAD (1G5J), FADD and NF-κB (1SVC) was modified with the "protein preparation wizard" by deleting the substrate cofactor and crystallographically observed water molecules. The prepared protein receptor grid files and the minimized ligand database were given as input in the virtual screening workflow protocol. Then single low energy 3D structure of ligands with correct chiralities was docked with the binding site using the 'extra precision' Glide algorithm in Schrodinger.

MTT assay

Prostate cancer (PC-3) cell line was obtained from National Centre for Cell Science (NCCS), Pune, India. The cells were grown in T25 culture flasks containing DMEM supplemented with 10% FBS, L-Glutamine (200mM) and penicillin/streptomycin/ Fungizone (10,000units/ mL, 10,000μg/mL, 25μg/mL) solutions. Cells were maintained at 37ºC in a humidified atmosphere containing 5%CO_2. DMEM, PBS were purchased from Hyclone (Thermo Scientific, USA), while Antibiotic-Antimycotic (100×) and FBS were procured from Gibco (Thermo Scientific, USA). Hesperetin was purchased from Cayman Chemicals, USA. All other chemicals and plasticwares (SPL, Korea) used were of cell culture grade.

Cytotoxicity was assessed by MTT method as dying cells exhibit a sharp decrease in MTT reduction activity (Mosmann, 1983; van de Loosdrecht et al., 1994). Briefly, cells were grown in 48-well plates in medium with or without hesperetin at various concentrations from 0-100μM. At the end of 24 and 48h, they were incubated with 200μL of yellow tetrazolium MTT (3- (4, 5-dimethylthiazolyl-2)-2, 5-diphenyltetrazolium bromide) (5mg/mL) in PBS at 37°C for 2 hours. The supernatant was removed, then formazan crystals were solubilized in DMSO and stirred for 10min at room temperature. The optical density was read at 570nm using an ELISA plate reader (Synergy HT Multi-Mode Microplate Reader, BioTek, USA). The cell viability was calculated using the formula: *Percentage of growth inhibition=(A_{570} of treated cells/A_{570} of control cells)×100*

Real time-PCR analysis

mRNA expression levels of *BAD, BAX* and BCL_{XL} were examined using realtime RT-PCR. The total RNA was isolated using Trizol (Invitrogen, USA). Total RNA (1μg) from each sample was reverse transcribed using a commercial iScript cDNA synthesis kit according to the manufacturer's protocol (Bio-Rad, USA). Real time-PCR was carried out in Bio-Rad CFX-96 using IQ SYBR Green PCR master mix kit (Bio-Rad, USA). The sequence of primers together with their expected amplified fragments are given in Table 1. The PCR was carried out in a total volume of 20μL including 0.25μM of forward and reverse primers. The PCR conditions were 95ºC for 10min, followed by 40 cycles of denaturation at 95ºC for 10s, annealing at 58ºC for 30s and extension at 72ºC for 30s. Fluorescent data were acquired during each extension phase. After 40 cycles a melting curve was generated by heating the sample to 95ºC programmed for 0s followed by cooling down to 55ºC for 5s and slowly heating the samples at 0.1ºC/s to 95ºC, while the fluorescence was measured continuously. Fast loss of fluorescence is observed at the denaturing/melting temperature of a DNA fragment, which is a unique feature of that fragment (Ririe et al., 1997). The data was analysed using Bio-Rad CFX manager software. The results were displayed as relative RNA levels expressed in arbitrary units which were calculated using comparative method based on ΔC_T values (Schmittgen and Livak, 2008). Reactions were carried out in triplicate and the mRNA expression was normalized against *CYC-A* as an internal control.

Western blot analysis

After 24h treatment period, cells were lysed using RIPA buffer containing 1× protease inhibitor cocktail (Sigma, USA) following which protein concentrations were measured using Lowry's method (Lowry et al., 1951). Cell lysates (20-50μg) were electrophoresed in 12% SDS polyacrylamide gel and then transferred to PVDF membranes. The membranes were incubated with primary antibodies against BAX, BCL_{XL}, NF-κB and β-Actin (1:1000) (Santa Cruz, USA) in Tris-buffered saline. After being washed, the membranes were incubated with HRP-conjugated goat-anti mouse IgG (1:5000) or HRP-conjugated goat-anti rabbit IgG (1:5000) accordingly. Protein bands were detected using chemiluminescence system (Rapid ECL detection kit, Merck, USA) and quantified using Chemi Doc XRS

Table 1. List of Primers

Gene	Primer Sequence 5'→3'	Product size	Reference
BAX	F- GCTGGACATTGGACTTCCTC	168bp	Elumalai
	R- CTCAGCCCATCTTCTTCCAG		et al., 2012
BAD	F- CCTCAGGCCTATGCAAAAAG	120bp	Elumalai
	R- AAACCCAAAACTTCCGATGG		et al., 2012
BCL_{XL}	F- GGCTGGGATACTTTTGTGGA	131bp	Elumalai
	R- AAGAGTGAGCCCAGCAGAAC		et al., 2012
CYC-A	F- GTGGTGTTTGGCAAAGTGAA	116bp	Vladic-Stjernholm
	R- TCGAGTTGTCCACAGTCAGC		et al., 2009

Table 2. Interaction Profile for BAX, BAD, FADD, BCL_{XL}, BCL_2 and NF-κB

Complex	GScore	Lipophilic EvdW	PhobEn	HBond	Electro	Sitemap	Phobic Penal
Hesperetin vs *BAX*	-4.55	-2.81	-0.24	-1.02	0	-0.08	0
Hesperetin vs *BAD*	-1.71	-1.29	0	-0.6	-0.95	0	1.54
Hesperetin vs *FADD*	-7.28	-3.8	0	-2.2	-0.62	-0.25	0
Hesperetin vs BCL_{XL}	-2.35	-4.15	-0.12	-0.82	0	-0.23	2.23
Hesperetin vs BCL_2	-7.1	-4	0	-2.5	-0.68	-0.25	2.29
Hesperetin vs *NF-κB*	**-7.48**	**-4.9**	**-0.15**	**-2.7**	**-0.72**	**-0.29**	**2.25**

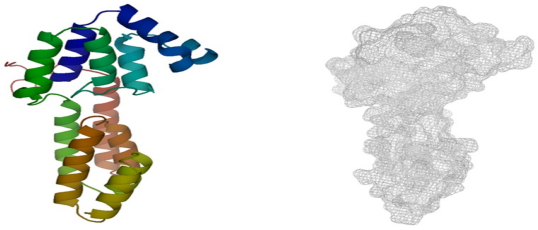

Figure 2. Modelled Structure of FADD Using Schrodinger Suite

Imaging System (Bio-Rad, USA).

Statistical analysis

Statistical analysis was performed using Graph Pad prism software (version 5) by using nonlinear regression analysis. IC_{50} values were calculated from dose response curves from six individual values. For expression analysis and western blot the experiments were repeated thrice. Level of significance was checked by using one-way ANOVA followed by Newman-Keuls test. $p<0.05$ was considered statistically significant.

Results

Docking studies

To investigate the detailed intermolecular interactions between hesperetin and its target protein, an automated docking program Glide (version 5.5) was used. The model of FADD (NP_003815.1) was generated based on the template Triosephospate isomerase of *Vibrio marinus* (PDB ID: 1AW1) (Figure 2). Three-dimensional structure data for the other target proteins was obtained from the PDB entry 1G5J, 1R2D, 1F16, 2O2F, 1SVC. Processing of the proteins included the deletion of the co-crystallized ligand and the solvent molecules as well as the addition of hydrogen atoms. Molecular docking revealed the interaction of hesperetin with the active site of target proteins FADD, BCL_{XL}, BAX, BAD, BCL_2 and NF-κB. All the protein–ligand complexes possessed multiple hydrogen bonds. On the basis of G-score parameter the binding affinity of ligand towards receptors was determined (Table 2). The higher negative value of glide score indicates a greater binding affinity of the ligand with receptor. When compared to the other target proteins, hesperetin showed high affinity towards NF-κB with glide score of -7.48KJ/mol. The Lipophilic EvdW is the lipophilic term derived from hydrophobic grid potential and fraction of the total protein-ligand vdW energy was very low for NF-κB (-4.9) when compared with other proteins. The HBond which is the Chem score H-bond pair was also low in NF-κB with score of -0.29. Electro, the

Table 3. Hesperetin Interaction with BAX, BAD, FADD, BCL_{XL}, BCL_2 and NF-κB

Residues		Receptor atom	Ligand atom	Distance
NF-κB vs Hesperetin	ARG59	N	O	2.98
	ILE 142	O	N	2.99
		O	O	2.6
Apoptosis regulator BCL_2 receptor vs Hesperetin				
	ARG104	H	O	2.69
	ARG107	H	O	2.95
		N	O	3
	ASP108	H	O	2.6
BAX vs Hesperetin	MET99	H	O	2.38
	ASP98	H	O	2.34
	TRP139	O	H	2.04
BAD vs Hesperetin	ARG307	H	O	1.82
	GLU311	O	H	1.6
	ARG314	H	O	2.17
BCL_{XL} vs Hesperetin	GLN19	H	O	1.63
	SER18	O	H	2.25
	SER14	H	O	1.71
FADD vs Hesperetin	GLU154	O	H	2.04
	ALA156	O	H	2.16
	GLY93	H	O	2.12
	GLU51	O	H	2.53

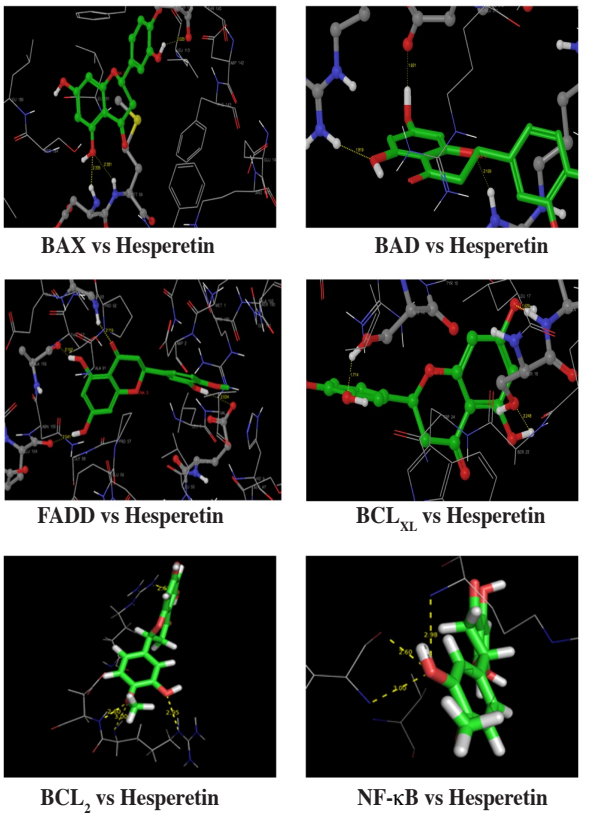

Figure 3. Interactions of Hesperetin with Pro-and Anti-Apoptotic Proteins

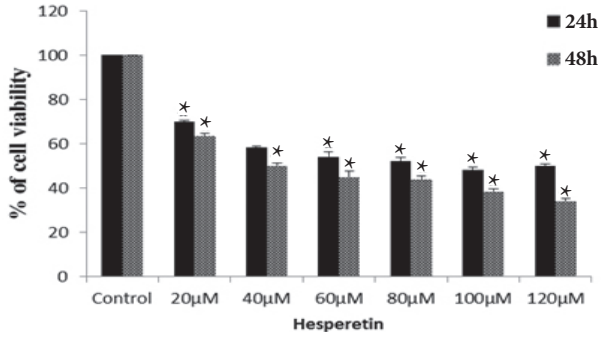

Figure 4. Effects of Hesperetin on PC-3 Cell Viability. Each Bar represents the Mean±SEM of six independent observations. '*' represents statistical significance between control vs hesperetin-treated groups at p<0.05 level using Newman-Keul's test

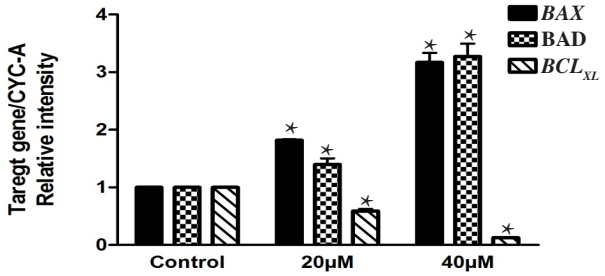

Figure 5. mRNA Expression of *BAX*, BAD and BCL_{XL} Normalized with CYC-A as an Internal Control. '*'represents statistical significance between control vs hesperetin–treated groups at p<0.05 level using Newman-Keul's test

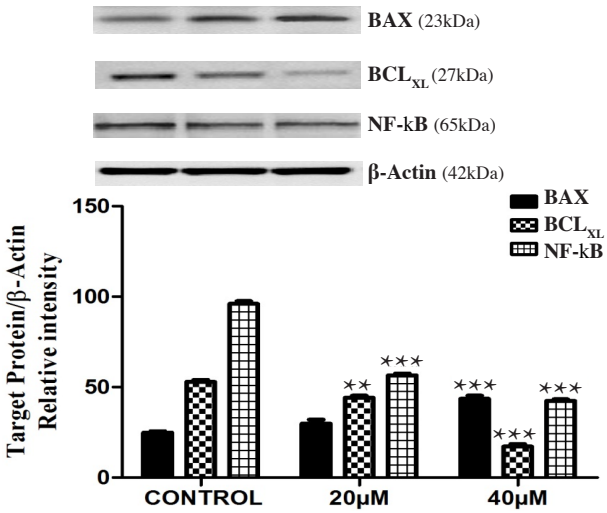

Figure 6. Western Blot Analysis of BAX, BCL_{XL} and NF-kB Normalized with β-Actin. L1-Control, L2-20μM and L3-40 μM. Bottom panel shows protein expression relative to that of β-Actin. '**' and '***'represents statistical significance between control vs hesperetin-treated groups at p<0.01 and p<0.001 level using Newman-Keul's test

electrostatic reward for the ligand protein interaction was low in BCL_2 (-0.68) and NF-κB (-0.72) when compared with the other proteins.

The conformations of the lead compound (hesperetin) binding to the target proteins and the hydrogen-bond interactions were analysed (Figure 3). The docking results for hesperetin against target proteins and their interaction details are given in Table 3. Hesperetin directly binds to ARG59 and ILE142 forming three high energy bonds with the DNA binding domain RHD (Rel Homology domain) of NF-κB (Ghosh et al., 1995; Xiao and Fu, 2011), thereby inhibiting NF-κB from binding to the DNA.

MTT assay

The cytotoxic effects of hesperetin in human prostate cancer PC-3 cells were assessed using MTT assay. A significant decrease was observed in the percentage of viable cells following treatment with different concentrations of hesperetin after 24h and 48h ($p<0.05$) (Figure 4). IC_{50} values of hesperetin in PC-3 cells after 24 and 48h of exposure were determined to be 90 and 40μM, respectively. Based on the viability trend 20 and 40μM for 24h were chosen as low and high dose respectively for subsequent assays.

Expression analysis of apoptotic genes

The expression of apoptotic genes like *BAX*, *BAD*, and BCL_{XL} with *CYC-A* as internal control in hesperetin-treated and control cells were analysed. There was significant increase in the expression of *BAX* and *BAD* genes by 1.8- and 1.4-fold at 20μM concentration respectively and 2.9- and 3.1-fold increase at 40μM concentration respectively in hesperetin-treated PC-3 cells when compared with control cells. In contrast, there was a significant decrease in the expression of BCL_{XL} 0.5- and 0.12- fold change in hesperetin-treated cells which ultimately drives the cells towards apoptosis (Figure 5). The western blot analysis also showed similar trend in BAX and BCL_{XL} protein levels as that of gene expression (Figure 6). The level of NF-κB was also decreased when treated with hesperetin (Figure 6).

Discussion

Abnormal proliferation of cells results from mutations or alterations in the expression of genes involved in apoptotic pathways. Cell death mediated by cytotoxic chemotherapy and radiation therapy in cancer is through endogenous apoptotic mechanisms. Activated BAX along with other pro-apoptotic proteins like BAD and BAK leads to oligomerization and permeablization of the mitochondrial membrane either by rupture or by formation of specific channels in the membrane, which leads to cytochrome-c release eventually resulting in activation of caspase cascade (Liu and Huang, 2011). BCL_{XL} inhibits this process by two different models. In one, BCL_{XL} binds to an activator (tBID), thereby preventing BAX activation. In the second, BCL_{XL} binds directly to the activated BAX resulting in preventing oligomerization (Billen et al., 2008). RT-PCR and Western blot assays revealed that hesperetin significantly down-regulated the expression of BCL_{XL} mRNA and protein in PC-3 cells. Hesperetin treatment also increased the *BAX* levels. Since PC-3 cells have relatively low expression of BCL_2 when compared with BCL_{XL} expression profile (Yamanaka et al., 2005), BCL_2 was not determined in the present study. Increased level of BAX would result in oligomerization and permiablization in the mitochondrial membrane and release of cytochrome-c from the mitochondria. The release of cytochrome-c would in turn trigger caspase

cascade-mediated apoptosis in hesperetin-treated PC-3 cells. Treatment with various cancer drugs has been reported to either upregulate BAX or decrease the BCL_2 protein level resulting in mitochondrial mediated apoptosis (Elmore, 2007).

The transcription factor nuclear factor κ*B* (NF-κB) regulates the expression of both antiapoptotic and proapoptotic genes. NF-κB is a family of closely related protein dimers that bind to a common sequence motif in DNA the κB site. The link between NF-κB and cancer came to light by the identification of p50 subunit (v-REL), a member of the reticuloendotheliosis (REL) family of viruses. Under resting condition, NF-κB dimers reside in the cytoplasm. NF-κB is activated by various signals like free radicals, inflammatory stimuli, cytokines, carcinogens, tumor promoters, endotoxins, γ-radiation, ultraviolet light, and X-rays. Upon activation, it gets translocated to the nucleus, where it induces the expression of many genes that suppresses apoptosis and induces cell survival. The target genes activated by NF-κB like cyclin D1, BCL_2, BCL_{XL}, matrix metalloproteinases (MMPs) and VEGF are very important for cellular transformation, cell proliferation, invasion, migration and metastasis (Dolcet et al., 2005; Perkins, 2012). NF-κB inhibition drives the cell towards apoptosis since the expression of all cell survival genes are decreased. Moreover, Hesperetin was reported to induce cell cycle arrest in G1 phase by decreasing the protein levels of NF-κB in MCF-7cell line (So et al., 1997). Downregulation of NF-κB by hesperetin leads to decrease in the cell survival gene BCL_{XL} and increase in *BAX* resulting in mitochondria-mediated apoptosis in PC-3 cell line. *In silico* docking studies confirmed the binding of hesperetin to DNA binding domain of NF-κB. This leads to prevention of expression of NF-κB mediated cell survival genes. It is pertinent to note that hesperetin has greater binding affinity within the DNA binding domain of NF-κB in comparison with the other pro- and anti-apoptotic proteins. These *in silico* findings are well supported by *in vitro* analysis of hesperetin with PC-3 cells. In conclusion hesperetin may be employed clinically as an anticancer drug. However research using *in vivo* models is needed to further clarify its underlying mechanism(s) of activity.

Acknowledgements

The authors are grateful to Prof. M. Michael Aruldhas, Head of the department of Endocrinology, University of Madras, for permitting the use of Real-Time PCR and Chemi-Doc system in his laboratory. The financial assistance from UGC-BSR to Sambantham is greatly acknowledged.

References

Billen LP, Kokoski CL, Lovell JF, Leber B, Andrews DW (2008). Bcl-XL inhibits membrane permeabilization by competing with *Bax*. *PLoS Biol*, **6**, 147.

Borradaile NM, Carroll KK, Kurowska EM (1999). Regulation of HepG2 cell apolipoprotein B metabolism by the citrus flavanones hesperetin and naringenin. *Lipids*, **34**, 591-8.

Choi EJ (2007). Hesperetin induced G1-phase cell cycle arrest in human breast cancer MCF-7 cells: involvement of CDK4 and p21. *Nutr Cancer*, **59**, 115-9.

Choi EJ (2008). Antioxidative effects of hesperetin against 7, 12-dimethylbenz(a)anthracene-induced oxidative stress in mice. *Life Sciences*, **82**, 1059-64.

Dolcet X, Llobet D, Pallares J, Matias-Guiu X (2005). *NF-κB* in development and progression of human cancer. *Virchows Arch*, **446**, 475-82.

Elmore S (2007). Apoptosis: a review of programmed cell death. *Toxicol Pathol*, **35**, 495-516.

Elumalai P, Gunadharini DN, Senthilkumar K, et al (2012). Induction of apoptosis in human breast cancer cells by nimbolide through extrinsic and intrinsic pathway. *Toxicol Lett*, **215**, 131-42.

Ghosh G, van Duyne G, Ghosh S, Sigler PB (1995). Structure of *NF-κB* p50 homodimer bound to a kB site. *Nature*, **373**, 303-10.

Jemal A, Bray F, Center MM, et al (2011). Global Cancer Statistics. *CA Cancer J Clin*, **61**, 69-90.

Leelavinothan P, Kalist S (2011). Beneficial effect of hesperetin on cadmium induced oxidative stress in rats: an *in vivo* and *in vitro* study. *Eur Rev Med Pharmacol Sci*, **15**, 992-1002

Liu D, Huang Z (2011). Synthetic peptides and non-peptidic molecules as probes of structure and function of Bcl-2 family proteins and modulators of apoptosis. *Apoptosis*, **6**, 453-62.

Lowry OH, Rosebrough NJ, Farr AL, Randall RY (1951). Protein measurement with the Folin–phenol reagent. *J Biol Chem*, **193**, 265-75.

Mosmann T (1983). Rapid colorimetric assay for cellular growth and survival: application to proliferation and cytotoxicity assays. *J Immunol Methods*, **65**, 55-63.

Nalini N, Aranganathan S, Kabalimurthy J (2012). Chemopreventive efficacy of hesperetin (citrus flavonone) against 1,2-dimethylhydrazine-induced rat colon carcinogenesis. *Toxicol Mech Methods*, **22**, 397-408.

Orallo F, Alvarez E, Basaran H, Lugnier C (2004). Comparative study of the vasorelaxant activity, superoxide-scavenging ability and cyclic nucleotide phosphodiesterase-inhibitory effects of hesperitin and hesperidin. *Nauyn-Schmeideberg's Arch Pharmacol*, **370**, 452-63.

Perkins ND (2012). The diverse and complex roles of *NF-κB* subunits in cancer. *Nat Rev Cancer*, **12**, 121-32.

Ririe KM, Rasmussen RP, Wittwer CT (1997). Product differentiation by analysis of DNA melting curves during polymerase chain reaction. *Anal Biochem*, **245**, 154-60.

Schmittgen TD and Livak KJ (2008). Analyzing real-time PCR data by the comparative CT method. *Nature Protocols*, **3**, 1101-8.

So FV, Guthrie N, Chambers AF, Carroll KK (1997). Inhibition of proliferation of estrogen receptor-positive MCF-7 human reast cancer cells by flavonoids in the presence and absence of excess estrogen. *Cancer Lett*, **112**, 127-33.

Tanaka T, Makita H, Kawabata K, et al (1997). Chemoprevention of azoxymethane-induced rat colon carcinogenesis by the naturally occurring flavonoids, diosmin and hesperidin. *Carcinogenesis*, **18**, 957-65.

van de Loosdrecht AA, Beelen RH, Ossenkoppele GJ, Broekhoven MG, Langenhuijsen MM (1994). A tetrazolium-based colorimetric MTT assay to quantitate human monocyte mediated cytotoxicity against leukemic cells from cell lines and patients with acute myeloid leukemia. *J Immunol Methods*, **174**, 311-20.

Vladic-Stjernholm Y, Vladic T, Blesson CS, Ekman-Ordeberg G, Sahlin L (2009). Prostaglandin treatment is associated with a withdrawal of progesterone and androgen at the receptor level in the uterine cervix. *Reprod Biol Endocrinol*, **7**, 116.

Xiao G, Fu J (2011). *NF-κB* and cancer: a paradigm of Yin-Yang.

Am J Cancer Res, **1**, 192-221.
Yamanaka K, Rocchi P, Miyake H, et al (2005). A novel antisense oligonucleotide inhibiting several antiapoptotic Bcl-2 family members induces apoptosis and enhances chemosensitivity in androgen-independent human prostate cancer PC3 cells. *Mol Cancer Ther*, **4**, 1689-98.